

# Weighted calculation for membrane permeability of nanofiltration and reverse osmosis

Mehdi Metaiche

PM3E Laboratory, University of Bouira, Bouira, Algeria,

Email: Metiche022000@yahoo.fr

## Abstract

*The objective of this work is to present a method for determining water and salt permeability of nanofiltration (NF) and reverse osmosis (RO) membranes.*

*This method is based on the Van der Meer algorithm for calculating transfers across NF and RO membranes for different types and geometries of modules. The algorithm was developed for a weighted calculation of permeability. The weighting elements are: elementary membrane surface, transmembrane pressure, pressure drop and concentration gradient.*

*The results obtained through the exploitation of the experimental data are satisfactory.*

**Keywords:** algorithm, membrane, nanofiltration, reverse osmosis, permeability.

## I. Introduction

Permeability of reverse osmosis and nanofiltration membranes is an important parameter which has to be calculated accurately enough to lead to reliable transfer values which in turn are fundamental for membrane systems calculation or design.

The current method for the calculation of membrane permeability is an approximative one and is based on a number of simplifications. However the resulting transfers usually show certain deviations compared to the experimental values.

Consequently in the present work a weighting method for the evaluation of the permeability of reverse osmosis and nanofiltration membranes was proposed, considering pure and salted water and with the main objectives of a good characterization of the membranes and a better modeling of the membrane transfer.

This study was carried out for specified and well-detailed cases: Dow FilmTec SW30HR380 spiral reverse osmosis membranes for different configurations of membrane networks and for different operating conditions.

The assessment of membrane permeability values has attracted the attention of many researchers. In the literature, some permeability values for this type of membrane can be found and are shown in Table 1.

Table 1 : Permeability values of SW30HR380 membrane, from literature.

Pure water permeability	Unit	Salt permeability	Unit	Reference
$2.7 \cdot 10^{-9}$	kg/m <sup>2</sup> /s/Pa	$2.3 \cdot 10^{-5}$	kg/m <sup>2</sup> /s	[1]
$2.5 \cdot 10^{-12}$	m/s/Pa	$2.5 \cdot 10^{-5}$	kg/m <sup>2</sup> /s	[2]
$2.33 \cdot 10^{-12}$	m/s/Pa	$2.21 \cdot 10^{-8}$	m/s	[3]
$2.58 \cdot 10^{-12}$	m/s/Pa	$2.22 \cdot 10^{-8}$	m/s	[3]
$2.33 \cdot 10^{-12}$	m/s/Pa	$1.88 \cdot 10^{-8}$	m/s	[3]
$2.24 \cdot 10^{-12}$	m/s/Pa	$1.84 \cdot 10^{-8}$	m/s	[3]
$3.00 \cdot 10^{-12}$	m/s/Pa	$1.7 \cdot 10^{-8}$	m/s	[4]

The most commonly used units for permeability are m/s/Pa for the case of pure water, and m/s for salt presence.

This study consists of calculating the permeability by the weighting method, and comparing them with those calculated by the approximate method, and those derived from literatures. The calculation; is based on the exploitation of experimental measurements on Dow FilmTec SW30HR380 spiral membranes.

## II. Geometry of spiral membranes

The spiral membranes of nanofiltration and reverse osmosis were formed by a separating membrane film with a thickness of about 150 nm, associated with one to two thicker resistant layers. The selective transport took place at the level of the separative film. The role of the other layers was only to support and improve the resistance. All of these two or three layers formed the membrane sheet. Each sheet was

folded to form a leaf (sandwich arrangement of flat sheet, membranes placed back-to-back). The spacer system (feed-retentate) was placed between the two parts of the leaf to create a space flow and passage of the liquid to be separated. A set of leaf was stacked and wrapped around a central tube that would convey the permeate flow. Another spacer system (permeate) was placed between each two leaves. The membrane leaves then took a spiral shape if a section perpendicular to the central tube (collector) was considered. All of these elements were mounted in a pack to form a membrane module. A set of modules mounted in series (the retentate from one module is the supply to the next), formed what the tube of pressure which would be associated with a high pressure pump for supplying it with pressurized liquid. The spacers were formed by crossing the filaments to form a network.

The feed and retentate flow took place in the inter-leaf space where the filament network was placed. It was a tangential flow compared to the winding of the membranes.

The permeate flow was normal to the membrane area, and then ran in the space between each two sheets, to join through the spiral path, the central tube (collector).

### III. Membrane transfer

The treatment of the membrane transfer phenomenon, for an aqueous solution containing salts; can be approached as two separate phenomena: the phenomenon of water transport and the phenomenon of salt transfer [5-10].

Considering a membrane sheet, having  $l$  as length,  $w$  as width, and  $e$  as thickness, surmounted by a spacer to form flow channels (feed side) in the  $x$  direction for the concentrated water, which infiltrated in the  $z$  direction, then flows in the flow channels (permeate side) in  $y$  direction (see Figure 1).

The Darcy model for the transfer of water through the membrane (porous medium) was adopted, and then flow of pure water was written as the product of the gradient of the pressure and a coefficient  $A'$ :

$$J_{w(x,y)} = A' \frac{dP}{dz} \quad (1)$$

Letting  $A' = A.e$  such that  $e$  was the membrane thickness, led to:

$$J_{w(x,y)} = A.e \frac{dP}{dz} \Rightarrow dP = \frac{J_{w(x,y)}}{A.e} dz \quad (2a)$$

$$\Rightarrow d(P - \sigma.\pi) = \frac{J_{w(x,y)}}{A.e} dz \quad (2b)$$

Where  $\sigma$ : is the reflection coefficient (Staverman coefficient).

$\pi$ : Osmotic pressure.

Integrating between the two membrane sides (feed/membrane interface side, and permeate side), led to:

$$\int d(P - \sigma.\pi) = \int \frac{J_{w(x,y)}}{A.e} dz \quad (3a)$$

$$\Rightarrow (P_{m(x,y)} - P_{p(x,y)}) - \sigma (\pi_{m(x,y)} - \pi_{p(x,y)}) = \frac{J_{w(x,y)}}{A.e} e \quad (3b)$$

$$\Rightarrow J_{w(x,y)} = A. \left( (P_{m(x,y)} - P_{p(x,y)}) - \sigma (\pi_{m(x,y)} - \pi_{p(x,y)}) \right) \quad (3c)$$

And since the pressure on the feed/membrane interface side is equal to the feed pressure  $P_m = P_f$ ; so we get for a reflection coefficient equal to unity; at every point  $(x, y)$ :

$$J_{w(x,y)} = A. \left[ (P_{f(x,y)} - P_{p(x,y)}) - (\pi_{m(x,y)} - \pi_{p(x,y)}) \right] \quad (4)$$

Where  $A$  is the pure water permeability of the membrane.

To describe the osmotic pressure for dilute solutions, we adopt the Van't Hoff model according to the following form [11, 12]:

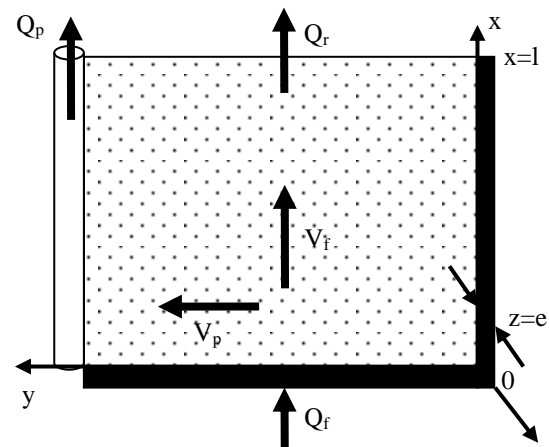


Figure 1 : Flow diagram around the membrane sheet : on the sheet the fluid flows in direction feed / retentate, and under the sheet ; flows in permeate direction towards the collector

$$\pi(Pa) = \frac{i.R.T.C}{Ms} \quad (5)$$

Where  $i$ : is the number of species (water + salt) ;  $i=2$ .

R : gas constante ;  $R=8.314472 \text{ m}^3.\text{Pa}/\text{K}.\text{mol}$ .  
 Ms: molar mass of mixture (water and salts) ;  $M_s=58.8.10^{-3} \text{ kg/mol}$ .  
 T : temperature ( $^{\circ}\text{K}$ ).  
 C : concentration ( $\text{kg}/\text{m}^3$ ).

And we will have in every point (x, y):

$$\pi_{m(x,y)} - \pi_{p(x,y)} = i. R. T (C_{m(x,y)} - C_{p(x,y)}) / M_s \quad (6)$$

The flow of a viscous fluid (as water) always generates a pressure loss, whose pressure gradient in the feed channel is given by the Darcy-Weisbach model as the ratio between the product of the square of the fluid velocity  $V_f$ ; fluid density  $\rho_f$ , the loss pressure coefficient  $\lambda_f$ , and the double of hydraulic diameter  $d_{hf}$  :

$$\frac{dP_f}{dx} = \frac{\lambda_f \rho_f}{2d_{hf}} V_f^2 \quad (7)$$

For a laminar flow  $\lambda_f = \frac{64}{Re_f}$ ; where  $Re_f$  is the Reynolds number in the feed channel which gives by:  $Re_f = \frac{V_f \cdot d_{hf}}{\nu_f}$ ; where  $\nu_f$  : kinematic viscosity of the fluid in the feed channel; it is equal to the ratio between the dynamic viscosity and the fluid density in the same channel:  $\nu_f = \frac{\mu_f}{\rho_f}$ .

A substitution gives:

$$\frac{dP_f}{dx} = \frac{32 \cdot \mu_f}{d_{hf}^2} V_f \quad (8)$$

In addition, we have  $V_f = \frac{dQ_f}{dS_{cf}}$ , and by substitution, we obtain:

$$\frac{dP_f}{dx} = \frac{32 \cdot \mu_f}{d_{hf}^2} \frac{dQ_f}{dS_{cf}} \quad (9)$$

Let's assume by definition that for a flow channel having  $dy$  as width; the hydraulic diameter represents four times the ratio of the flow section and the wet flow perimeter [13], and this wet perimeter represents the sum of twice the channel width  $dy$  and twice the channel thickness channel  $h_{sf}$ ; and we will have :

$$\begin{aligned} d_{hf} &= 4 \cdot \frac{dS_{cf}}{dp_f} \Rightarrow dS_{cf} = \frac{d_{hf} \cdot dp_f}{4} \\ &= \frac{d_{hf} \cdot 2(dy + h_{sf})}{4} \\ &= \frac{d_{hf} \cdot dy \left(1 + \frac{h_{sf}}{dy}\right)}{2} \approx \frac{d_{hf} \cdot dy}{2} \end{aligned} \quad (10)$$

Let  $d_{hf} = h_{sf}$  [1, 14], then:

$$\frac{dP_f}{dx} = \frac{64 \cdot \mu_f}{h_{sf}^3} \cdot \frac{dQ_f}{dy} = - \frac{64 \cdot \mu_f}{h_{sf}^3} \cdot \frac{dQ_p}{dy} \quad (11)$$

And as we already have :  $dQ_p = 2J_w \cdot dx \cdot dy$

$$\frac{dP_f}{dx} = - \frac{128 \cdot \mu_f}{h_{sf}^3} \cdot J_w \cdot dx \cdot \frac{dy}{dy} = - \frac{128 \cdot \mu_f}{h_{sf}^3} \cdot J_w \cdot dx \cdot \frac{\iint_S dx dy}{\iint_{S_{cf}} dx dy} \quad (12)$$

And by definition:  $\frac{\iint_S dx dy}{\iint_{S_{cf}} dx dy} = \frac{1}{\varepsilon_{cf}}$  therefore at every point:

$$\frac{dP_f}{dx} = - \frac{128 \cdot \mu_f(x,y)}{h_{sf}^3 \cdot \varepsilon_{cf}} \cdot J_w(x,y) \cdot dx \quad (13)$$

To obtain the permeate flow rate through an elementary membrane permeation area  $dS = dx dy$ , the following common definition (it was taken into account of the water passage through the two sheets that formed the leaf of membrane) was used:

$$J_w(x,y) = \frac{dQ_p}{2 \cdot dS} \Rightarrow \int dQ_p = \int J_w \cdot 2dS \quad (14)$$

$$Q_p = \int 2J_w(x,y) \cdot dy dx \quad (15)$$

The pressure gradient in the permeate channel is given according to the Darcy-Weisbach model and by analogy to the equation (3):

$$\frac{dP_p}{dy} = \lambda_{p(x,y)} \cdot \frac{\rho_p(x,y)}{2 \cdot d_{hp}} V_{p(x,y)}^2 \quad (16)$$

According to Schock and Miquel [13]:

$$\lambda_{p(x,y)} = 105 \cdot Re_{p(x,y)}^{-0,8} = 105 \cdot \left[ \frac{V_{p(x,y)} \cdot d_{hp}}{\nu_{p(x,y)}} \right]^{-0,8} \quad (17)$$

The flow velocity in the permeate channel  $V_p$  was not constant along y; but its function was given as:

$$\frac{dV_p}{dy} = \frac{dQ_p}{dy \cdot dS_{cp}} = \frac{dQ_p}{dy \cdot dx \cdot h_{sp}} \quad (18a)$$

since  $dQ_p = 2J_w(x,y) \cdot dx \cdot dy$ , then:

$$\frac{dV_p}{dy} = \frac{2J_w(x,y)}{h_{sp}} \cdot \frac{dx \cdot dy}{dy \cdot dx} = \frac{2J_w(x,y)}{h_{sp}} \cdot \frac{\iint_S dx dy}{\iint_{S_{cp}} dx dy} \quad (18b)$$

By definition,  $\frac{\iint_S dx dy}{\iint_{S_{cp}} dx dy} = \frac{1}{\varepsilon_{cp}}$

Where  $\varepsilon_{cp}$  is the porosity of permeate channel.

In every point (x, y) ; it can be written:

$$\frac{dV_p}{dy} = \frac{2J_w(x,y)}{h_{sp} \cdot \varepsilon_{cp}} \quad (18c)$$

With this analysis, the membrane transport of water was the first phenomenon and was well described by

the model.

For the second phenomenon, Fick's law was adopted to describe the transfer flux of salts across the membrane. This flux was nothing other than the product of the concentration gradient of salts by the coefficient B' as:

$$J_{s(x,y)} = B' \frac{dC}{dz} \quad (19)$$

Putting  $B' = B \cdot e$ , with e the membrane thickness, gives:

$$J_{s(x,y)} = B \cdot e \frac{dC}{dz} \Rightarrow dC = \frac{J_{s(x,y)}}{B \cdot e} dz \quad (20)$$

Integration between the two sides of the membrane (feed/membrane interface side, and permeate side), gives:

$$\int dC = \int \frac{J_{s(x,y)}}{B \cdot e} dz \Rightarrow (C_m - C_p) = \frac{J_{s(x,y)}}{B \cdot e} e = \frac{J_{s(x,y)}}{B} \quad (21a)$$

$$J_{s(x,y)} = B \cdot (C_{m(x,y)} - C_{p(x,y)}) \quad (21b)$$

with B the salt permeability of the membrane.

The equation (21b) can be written as:

$$J_{s(x,y)} = B \cdot (C_{m(x,y)} - C_{p(x,y)}) - (1 - \sigma) \bar{C}_s \cdot J_{w(x,y)} \quad (22)$$

Where  $\bar{C}_s$ : is the average concentration moyenne, and  $\sigma = 1$ .

To obtain the permeate concentration at all points, the following definition was used:

$$C_{p(x,y)} = \frac{J_{s(x,y)}}{J_{w(x,y)}} \quad (23)$$

A flow tangential to a selective membrane always generates a boundary layer of concentration, parallel and close to the membrane, slowing down the transfer. This boundary layer forms an interface between the membrane side and the free fluid layer. This phenomenon is called polarization of concentration. The concentration in this layer  $C_m$  increases in the x direction of the flow (see Figure 2). The relation which links this braking and this increase of the concentration can be described at all points, by the film theory model [15] as follows:

$$J_{w(x,y)} = k_{(x,y)} \cdot \ln \left[ \frac{C_{m(x,y)} - C_{p(x,y)}}{C_{0(x,y)} - C_{p(x,y)}} \right] \quad (24)$$

Where  $C_0$  is the salt concentration in the fluid outside the polarization layer (it is equal to that before entering on the membrane).

k: is the mass transfer coefficient; it represents the ratio between the product of Sherwood number Sh, the salt diffusivity in water D and the hydraulic diameter  $d_h$  :

$$k_{(x,y)} = Sh_{f(x,y)} \cdot \frac{D_{f(x,y)}}{d_{h_f}} \quad (25)$$

The Sherwood number is a combination of dimensionless numbers: Reynolds number Re and Schmidt number Sc; as follow:

$$Sc_{f(x,y)} = \frac{\nu_{f(x,y)}}{D_{f(x,y)}} = \frac{\mu_{f(x,y)}}{\rho_{f(x,y)} \cdot D_{f(x,y)}} \quad (26)$$

$$\Rightarrow Sh_{f(x,y)} = \alpha \cdot Re_{f(x,y)}^\beta \cdot Sc_{f(x,y)}^\gamma \quad (27)$$

We can admit the following values for the coefficients  $\alpha, \beta, et \gamma$  [13]:

$$\alpha = 0,04 ; \beta = 0,75 ; \gamma = 0,333$$

Therefore, the concentration in the boundary layer; will be given at every point in the flow, by:

$$C_{m(x,y)} = C_{p(x,y)} + (C_{0(x,y)} - C_{p(x,y)}) e^{\frac{J_{w(x,y)}}{k_{(x,y)}}} \quad (28)$$

And the thickness of the polarization boundary layer can be given by:

$$\delta_{f(x,y)} = \frac{D_{f(x,y)}}{k_{(x,y)}} \quad (29)$$

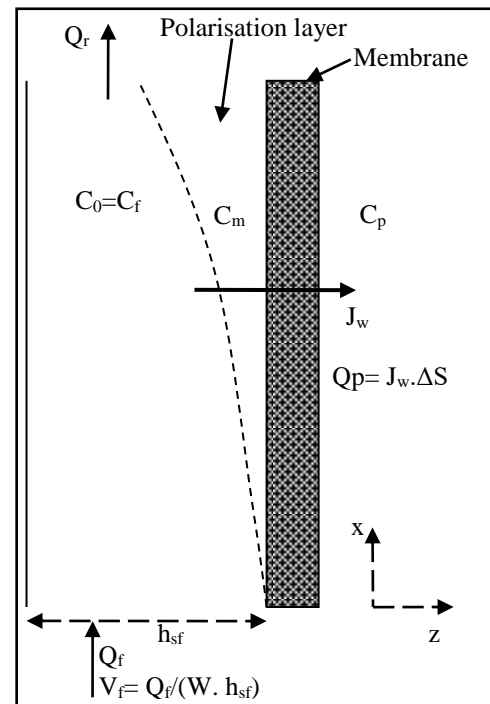


Figure 2: Positioning of the polarization layer

To finish with the description of the transfer model, it is necessary to note two questions:

i) Continuity of pure fluid and salts at any point in the flow and is expressed as follow:

$$Q_{f(x,y)} = Q_{p(x,y)} + Q_{r(x,y)} \quad (30)$$

$$Q_{f(x,y)} \cdot C_{f(x,y)} = Q_{p(x,y)} \cdot C_{p(x,y)} + Q_{r(x,y)} \cdot C_{r(x,y)} \quad (31)$$

ii) The water density, the solution (water + salts) viscosity, and the salt diffusivity in the water; can

obtained by the model at any point in the flow, depending on the temperature and the concentration. The following models were accepted according to [16, 17]:

$$\rho_{(x,y)} = 498,4. m. \mu(x,y) + \sqrt{248400. m^2 + 752,4. m. C_{(x,y)}} \quad (32)$$

$$\text{With } m = 1.0069 - 2.757. 10^{-4}. T(^{\circ}C) \quad (33)$$

$$\mu_{(x,y)} = 1.234. 10^{-3}. e^{\left[0,00212.C_{(x,y)} + \frac{1,965}{273,15+T(^{\circ}C)}\right]} \quad (34)$$

$$v_{(x,y)} = \frac{\mu_{(x,y)}(Pa. s)}{\rho_{(x,y)}} \quad (35)$$

$$D_{(x,y)} = 6,725. 10^{-9}. e^{\left[0,1546.10^{-3}. C_{(x,y)} - \frac{2,513}{273,15+T(^{\circ}C)}\right]} \quad (36)$$

#### IV. Resolution

To solve the transfer problem, two methods are possible: approximate method, and weighting method.

##### IV.1 Approximate method

This method is based on the simplification of the differential equations (Equations from 3 to 36) by some approximations, to reduce them to a simple and short calculation.

The membrane was considered as a single sheet having an active length  $l$  and active width  $w$ , so its area was  $S = l.w$ .

The concentration in the boundary layer has a mean value:

$$C_m = \frac{C_0 + C_r}{2} \quad (37)$$

Where  $C_r$ : is concentration at the outlet of the membrane.

The variation of the thickness of the polarization layer is linear.

The pressure loss is neglected. In the limit of the cases, it linked to the average velocity:

$$\frac{\Delta P_f}{\Delta x} = - \frac{64. \mu_f}{w. h_s f^3} \cdot \frac{Q_f + Q_r}{2} \quad (38)$$

The permeate pressure is constant and is equal to the atmospheric pressure. So the velocity is constant in the permeate channels, and there is no pressure loss.

The resolution algorithm is therefore:

1-Set the given data such as the total surface of the membrane (corresponding to a module or a pressure vessel), the temperature, the feed pressure, the permeate pressure, the feed flow rate, the permeate flow rate, the feed and the permeate concentration.

2-Use of the continuity equations to compute: the

concentrate flow rate and concentrate concentration, the concentration of the boundary layer, and the osmotic pressures in the boundary layer and in the permeate.

3-The membrane permeability will therefore be:

$$A = \frac{Q_p}{s. [(P_f - P_p) - (\pi_m - \pi_p)]} \quad (39a)$$

$$B = \frac{c_p. Q_p}{s. (C_m - C_p)} \quad (39b)$$

##### IV.2 Weighting method

This algorithm is based on the Van Der Meer algorithm [18] for calculating transfers, and the Taniguchi algorithm [16, 17] for the review of effect of temperature on membrane permeability.

The problem is therefore to solve the transfer problem whose solutions are known (flow rates, concentrations and pressures), and to weight and calculate the permeability based on these known solutions.

The calculation of the transfer is done by the numerical resolution of the system of differential equations (equations from 1 to 21), by the finite difference method (the multidimensional Runge-Kutta method is adopted), which requires the 2D discretization of the flow domain on finite element along the feed flow (concentrate) and along the permeate flow. The procedure consists in dividing the membrane in  $n$  increments according to  $y$  direction, and  $m$  increments according to  $x$  direction ( $m. \Delta x = w$  and  $n. \Delta y = l$ ) (see figure 3). A network of mesh of  $50 \times 50$  is considered; sufficient. The different types of boundary conditions and their values are summarized in Table 2.

Table 2 : Types and values of boundary conditions on a spiral membrane sheet

$V_f(x, y) = V_0$	$x = 0 \text{ et } 0 \leq y \leq W$
$C_f(x, y) = C_0$	$x = 0 \text{ et } 0 \leq y \leq W$
$P_f(x, y) = P_0$	$x = 0 \text{ et } 0 \leq y \leq W$
$V_p(x, y) = 0$	$y = 0 \text{ et } 0 \leq x \leq L$
$\frac{\partial C_p(x, y)}{\partial y} = 0$	$y = 0 \text{ et } 0 \leq x \leq L$
$\frac{\partial P_p(x, y)}{\partial y} = 0$	$y = 0 \text{ et } 0 \leq x \leq L$
$P_p(x, y) = 0$	$y = w \text{ et } 0 \leq x \leq L$

The following algorithm is adopted for the weighted calculation of permeabilities:

- 1-Having real values  $Q_{p0}$  and  $C_{p0}$ .
- 2- Set the values of A and B.

3-Calculate the transfer by the finite difference method in 2D. This calculation consists in setting the value of the permeate pressure at the closed end ( $y = 0$ ) of the permeate channel; pressures, concentrations, flows and velocities are calculated at any point in the mesh network by an iterative technique. The halting criteria will be when the conditions at the outlet (open end of the permeate channel 'end of membrane sheet':  $y = w$ ) are reached (the permeate pressure at this point 'in the collector tube' is atmospheric), with a precision chosen of  $10^{-5}$  and considered as sufficient. To make a new increment following the  $y$  direction, it is considered that its feed is the concentrate of the previous step (increment). Stopping calculations are performed once the last increment ( $n^{\text{th}}$ ) is calculated.

4-Calculate  $Q_{p\text{cal}}$  and  $C_{p\text{cal}}$ .

5-Calculate the permeabilities A and B:

$$A_{\text{cal}} = \frac{Q_{p0}}{\sum_{i=1}^n \sum_{j=1}^m \{2\Delta x \Delta y \cdot [(P_{f(i,j)} - P_{p(i,j)}) - (\pi_{m(i,j)} - \pi_{p(i,j)})]\}} \quad (40a)$$

$$B_{\text{cal}} = \frac{C_{p0} \cdot Q_{p0}}{\sum_{i=1}^n \sum_{j=1}^m \{2\Delta x \Delta y \cdot (C_{m(i,j)} - C_{p(i,j)})\}} \quad (40b)$$

6-Comparison:

IF  $Q_{p\text{cal}} = Q_{p0}$  and  $C_{p\text{cal}} = C_{p0}$ ; So :  $A = A_{\text{cal}}$  and  $B = B_{\text{cal}}$ ; the permeabilities are well calculated.

If no : if  $Q_{p\text{cal}} \neq Q_{p0}$  or  $C_{p\text{cal}} \neq C_{p0}$ ; put  $A = A_{\text{cal}}$  and  $B = B_{\text{cal}}$  and start again from step 3.

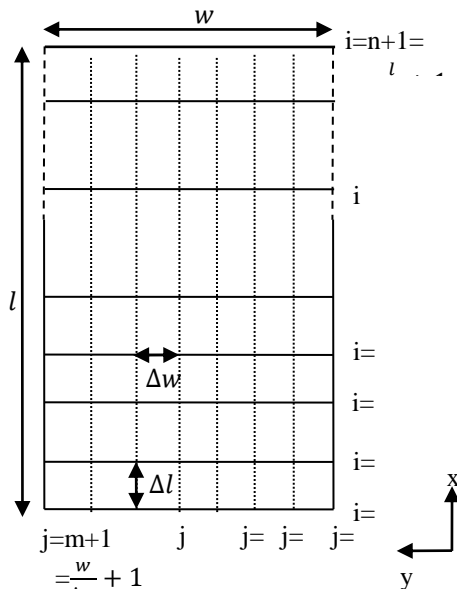


Figure 3 : Discretization of the flow domain around the membrane sheet

### V. Results and discussion

To demonstrate the efficiency and the utility of the weighting calculation algorithm for membrane

permeability, the case of reverse osmosis membranes of Dow FilmTec SW30HR380 type, was considered. The characteristics of this type of membrane are shown in Table 3.

The validation of the model was carried out considering nine measurement points, numbered from one to nine. For each measuring point configuration of the membrane network, temperature, pressure, flow rate, feed concentration, and flow rate and concentration of permeate were specified. The first point represented the manufacturer's own measurements made in tests on a single module: a single stage formed by a single pressure tube containing only one (1x1).

The following four points were experimental measurements performed on a network of six pressure tubes in parallel, each containing six modules in series (6x6). Points 3 and 5 showed the measurements made at the first module of each tube with respect to the permeate flow rate, while the permeation concentration was sought by the Desal code [19], so it's like the network is of the form 6x1. The last four represented measurements taken on the small mono-level desalination plant at Porto Santo Island (Portugal) [3]; the latter with a capacity of 1000 m<sup>3</sup>/d, was formed by twelve pressure tubes in parallel, each containing six modules in series (12x4). The data are presented in Table 4.

Table 3 : Characteristics of SW30HR380 membrane module

Number of leaf per module	13
Membrane active length (m)	0.8665
Membrane active width (m)	1.17
Thickness of feed spacer (mm)	0.84
Thickness of permeate spacer (mm)	0.52

The programming of the permeability weighting and of the approximate method algorithms was performed under a MATLAB code. A comparison of the results was made to show the differences between the two methods.

The calculation algorithm by weighting the membrane permeability; shows that the values of the permeability are lower than those; calculated by the approximate method: this observation is; valid for the pure water permeability A, and for the salt permeability B (see figures 4 and 5). This; can be explained by the power of the weighting method; which is more logical and precise. This precision depends on the numerical method used for the treatment of the differential equations, and the care provided for the discretization of the flow medium

Table 4: Measured parameters for the different considered points (SW30HR380 model)

Reference	Cp (g/l)	Qp (l/s)	Cf (ppm)	Qf (l/s)	Pf (bar)	T (°C)	Number of modules in each pressure vessel	Number of pressure vessel in membrane system	N° of point
[20]	0.096	0.266x1	32	3.328x1	55.2	25	1	1	1
[19]	0.38	0.72x6	42	2.0176x6	62.0	25	6	6	2
[19]	0.195	0.190x6	42	2.0176x6	62.0	25	1	6	3
[19]	0.395	0.631x6	42	2.0176x6	57.0	25	6	6	4
[19]	0.190	0.163x6	42	2.0176x6	57.0	25	1	6	5
[3]	0.287	0.58x12	38	1.8750x12	59.0	19	4	12	6
[3]	0.275	0.613x12	38	1.9083x12	59.0	19	4	12	7
[3]	0.264	0.55x12	38	1.6833x12	59.0	19	4	12	8
[3]	0.278	0.501x12	38	1.6250x12	57.1	19	4	12	9

and for the good description of the geometry of the

transfer domain. The different simplifications used by the approximate method are not sufficient. These have always led to values of permeabilities far from reality, which has posed real problems in the prediction, calculation and design models of membrane systems.

This difference is very remarkable for the permeability A (obtained by the approximation method) is almost four times that obtained by the weighting method, for the point n°4. This can be explained by the number of approximations made: three approximations on the water transport model (at the membrane surface, at the pressure loss level, and at the permeate pressure level), against a single approximation on the salt transfer models (at the concentration level in the boundary layer).

It is very clear that the value of the permeability A at the point n°1 is the highest relative to the other points, and the value of the permeability B at the same point is the lowest compared to the other points. The possible explanation is that the measurements concerning the point n°1 are; carried out by the manufacturer himself. The increase of A and the decrease of B shows that this type of membrane is more efficient compared to reality: the membrane is therefore more permeable to water and more selective to salts.

For the permeability A, the obtained values by the approximate method are in the same range of the values found in the literature (see Table 1):  $2.24 \times 10^{-12}$  to  $3.0 \times 10^{-12}$  m/s/Pa (with the exception from the point n°1), see Figure 4.

This shows that the approximate method is widely used to evaluate membrane performances by manufacturers. However the obtained values are overestimated compared to values from literature (almost equal to  $4.10^{-12}$  m/s/Pa) and B is lower.

The values of permeability A; calculated by the weighted method are lower than values derived from literature. They are below  $1, 5 \cdot 10^{-12}$  m/s/Pa (except the point n°1 where A that calculated by weighting method is around  $2.0 \cdot 10^{-12}$  m/s/Pa). The calculations commonly used for membrane transfer therefore consider permeability higher than reality, which has led to believe that the membranes are more permeable and efficient.

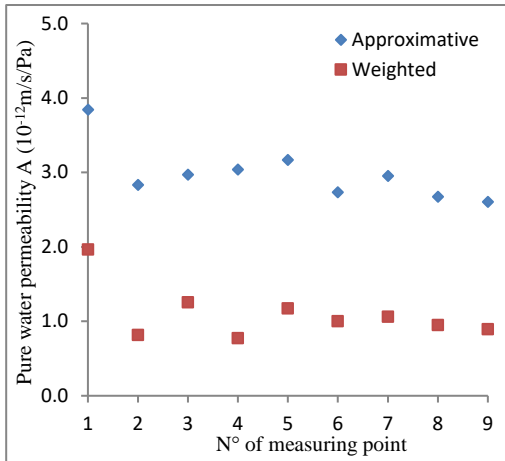


Figure 4 : Pure water permeability of the membrane for the different points.

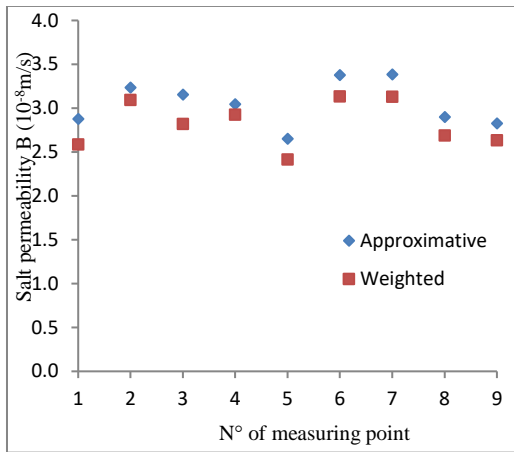


Figure 5 : Salt permeability of the membrane for the different points.

**VI. Conclusion**

A comparative study between the widely used approximative method for calculating membrane permeabilities, and the proposed weighting method was carried out.

The weighting method was based on the proper computation of the membrane transfer, by a fine modeling, a thorough consideration of the medium of the flow and the geometry of the separative domain, a correct choice of weighting and a robust algorithm for calculation.

The weighting method was more accurate (compared to the widely used approximate method), giving results close to the real permeability values for Reverse Osmosis and Nano Filtration membranes, and provided a useful tool for the computation, the prediction, the design, the characterization and the diagnosis of the membrane systems.

**VII. List of symbols**

A	Pure water permeability of membrane (m/s/Pa)
B	Salt permeability of the membrane (m/s)
C	Concentration (kg/m <sup>3</sup> )
D	Diffusivity of salt in water (m <sup>2</sup> /s)
<i>d<sub>h</sub></i>	Hydraulic diameter (m)
<i>e</i>	Membrane thickness (m)
<i>h<sub>s</sub></i>	Spacer thickness (channel) (m)
<i>i</i>	Number of species (-)
<i>J<sub>w</sub></i>	Water flux through the membrane (m/s)
<i>J<sub>s</sub></i>	Sal flux through the membrane (kg/m <sup>2</sup> /s)
<i>k</i>	Mass transfer coefficient (m/s)
<i>l</i>	Active length of membrane sheet (m)
<i>M<sub>s</sub></i>	Molar mass of mixture (water-salt) (kg/mol)
<i>P</i>	Pressure (Pa)
<i>p</i>	Wet perimeter (m)
<i>Q</i>	Flow rate (m <sup>3</sup> /s)
<i>R</i>	Gas constant (m <sup>3</sup> .Pa/K/mol)
<i>Re</i>	Reynolds number (-)
<i>S</i>	Area (m <sup>2</sup> )
<i>Sc</i>	Schmidt number (-)
<i>Sh</i>	Sherwood number (-)
<i>T</i>	Temperature (°K, °C)
<i>V</i>	Fluid velocity in spacer (m/s)
<i>w</i>	Active width of membrane sheet (m)
<i>x, y, z</i>	Space dimensions (m)
<i>δ</i>	Boundary layer thickness (m)
<i>ε</i>	Spacer porosity (-)
<i>λ</i>	Pressure loss coefficient (-)
<i>μ</i>	Dynamic viscosity (Kg/m/s)
<i>ν</i>	Kinematic viscosity (m <sup>2</sup> /s)
<i>π</i>	Osmotic pressure (Pa)
<i>ρ</i>	Fluid density (Kg/m <sup>3</sup> )
<i>σ</i>	Reflection coefficient (-)
<b>Indices</b>	
0	Free fluid
c	Channel
f	Feed
m	Boundary layer (membrane)
p	Permeate
r	Retentate
s	Salt
w	Water

**References**

[1] Yan-Yue Lu, Yang-Dong Hu, Xiu-Ling Zhang, Lian-Ying Wu, Qing-Zhi Liu, Optimum design of reverse osmosis system under different feed concentration and product specification, Journal of Membrane Science 287 (2007) 219–229.

[2] François Vince, François Marechal, Emmanuelle Aoustin, Philippe Bréant, Multi-objective optimization of RO desalination plants, Desalination 222 (2008) 96–118.

[3] Vitor Geraldes, Nuno Escorcio Pereira, and

- Maria Norberta de Pinho, Simulation and Optimization of Medium-Sized Seawater Reverse Osmosis Processes with Spiral-Wound Modules, *Ind. Eng. Chem. Res.* 2005, 44, 1897-1905.
- [4] Tahereh Kaghazchi, Mahdieh Mehri, Maryam Takht Ravanchi, Ali Kargari, A mathematical modeling of two industrial seawater desalination plants in the Persian Gulf region, *Desalination* 252 (2010) 135–142.
- [5] Katchalsky, A., and P. F. Curren, *Non-equilibrium Thermodynamics in Biophysics*, Harvard Univ. Press, Cambridge, MA (1981).
- [6] Kimura, S., Analysis of Reverse Osmosis Membrane Behaviors in a Long-Term Verification Test, *Desalination*, 100, 77 (1995).
- [7] Fukunaga, K., M. Matsukata, K. Ueyama, and S. Kimura, Reduction of Boron Concentration in Water Produced by a Reverse Osmosis Sea Water Desalination Unit, *MAKU (Memb.)*, 22, 211 (1997).
- [8] Ikeda, K., S. Kimura, and K. Ueyama, Characterization of a Nanofiltration Membrane Used for Demineralization of Underground Brackish Water by Application of Transport Equations, *MAKU (Memb.)*, 23, 266 (1998).
- [9] Anil Kumar and S. Deswal, Mathematical Modeling for Separation of Binary Aqueous Solution using Hollow Fiber Reverse Osmosis Module, *World Academy of Science, Engineering and Technology* 51 2009.
- [10] Aihua Ahu, Panagiotis D. Christofides, Yoram Cohen, Minimization of energy consumption for a two-pass membrane desalination: effect of energy recovery, membrane rejection and retentate recycling, *Journal of Membrane Science* 339 (2009) 126-137.
- [11] Marian G. Marcovecchio, Pi' o A. Aguirre, Nicola' s J. Scenna, Global optimal design of reverse osmosis networks for seawater desalination: modeling and algorithm, *Desalination* 184 (2005) 259–271.
- [12] John Palmeri et Mehdi Metaiche, Dessalement de l'eau de mer et des eaux saumâtres par Osmose Inverse et Nanofiltration: Théorie de transport, Modélisation et Processus de Simulation, Manuel de cours intensif de quatre jours, édité par the Middle East Desalination Research Center, Maskat, 2009 (246 p.).
- [13] Shock, G.; Miquel, A. Mass Transfer and Pressure Loss in Spiral Wound Modules. *Desalination* 1987, 64, 339
- [14] Nader M. A1-Bastaki, Abderrahim Abbas, Predicting the performance of RO membranes, *Desalination* 132 (2000) 181-187.
- [15] S. Sourirajan, *Reverse Osmosis*, Academic Press, New York, 1970.
- [16] Masahide Taniguchi and Shoji Kimura, Estimation of Transport Parameters of RO Membranes for Seawater Desalination, *AIChE Journal* October 2000 Vol. 46, No. 10.
- [17] Masahide Taniguchi, Masaru Kurihara, Shoji Kimura, Behavior of a reverse osmosis plant adopting a brine conversion two-stage process and its computer simulation, *Journal of Membrane Science* 183 (2001) 249–257.
- [18] W. G.J. van der Meer, I C. van Dijk, Theoretical optimization of spiral-wound and capillary nanofiltration modules, *Desalination* 113 (1997) 129-146
- [19] S. A. Avlonitis, M. Pappas, K. Moutesidis, unified model for the detailed investigation of membrane modules and RO plants performance, *Desalination* 203 (2007) 218–228.
- [20] Membrane Technical Information, [www.dow.com/liquidseps/service/lm\\_techinfo.htm](http://www.dow.com/liquidseps/service/lm_techinfo.htm).